scientific reports

Check for updates

OPEN

A flexible-spoke non-pneumatic tyre for manual wheelchairs

Otis Wyatt[1], Panagiotis Chatzistergos[2]✉, Nachiappan Chockalingam[1] & Evangelia Ganniari-Papageorgiou[3]

This study combines laboratory testing with computer modelling to demonstrate, for the first time, the applicability of flexible-spoke non-pneumatic tyre (FS-NPT) technology in wheelchairs. Like existing solid non-pneumatic tyres, FS-NPTs are puncture-proof and will reduce the burden of tyre maintenance. Unlike existing solid tyres, FS-NPT performance is based on the properties of flexible structures (spokes), such as honeycombs, which can deform to offer superior cushioning and return to their original shape upon unloading. The results presented here indicate that the geometry of these spokes can be tuned to replicate the vertical stiffness of existing pneumatic tyres commonly used in wheelchairs while achieving higher rotational stiffness and reduced mass. Vertical stiffness is directly linked to user comfort while increased rotational stiffness is associated with increased wheeling efficiency. Results also indicate that FS-NPTs can change their stiffness to become softer under increased loading. This unique characteristic could enable the development of tyres that are relatively stiff during wheeling (for better wheeling efficiency), and softer during impact loads for better cushioning (e.g. during pavement dismount). The demonstrated capacity for stiffness tuning could enable personalising wheelchair tyres to meet the specific needs of individual users.

Keywords Non-pneumatic tyres, Manual wheelchairs, Honeycomb, Finite element analysis

Previous reports demonstrate that wheelchair users desire a lightweight wheelchair that is comfortable and easy to propel[1]. As the standard manual wheelchair does not have a suspension system, tyre stiffness is crucial to achieving satisfactory levels of comfort. Moreover, wheelchair tyre selection is among the most important factors in reducing rolling resistance for more efficient wheeling[2].

To date, and for the last decades, wheelchair users can choose between two different types of tyres: pneumatic and solid non-pneumatic[3]. Out of these two, pneumatic tyres appear to have a relatively superior capacity to absorb impact and vibrations to mitigate discomfort and pain experienced by users when dismounting a pavement or when navigating over rough/uneven terrain [3,4]. Pneumatic tyres can also achieve good propulsion characteristics with relatively low resistance to rolling and good overall rolling efficiency[5]. However, these characteristics are directly related to tyre pressure which makes pressure maintenance extremely important[6]. Indeed, maintaining the wheeling efficiency of pneumatic tyres requires frequent control over tyre pressure which significantly increases the maintenance burden to users.

Pneumatic tyres can lose up to 40% of internal pressure per month leading to reduced wheeling efficiency[5] and can even cause secondary brake failure[7], emphasising the importance of regular pressure maintenance. Reduced wheeling efficiency increases the energy demand for users to propel themselves and increases the risk of injury by overexertion[5,8]. Furthermore, pneumatic tyres are prone to punctures[6]. This can be a devastating occurrence where an, otherwise independent, wheelchair user may become stranded due to the increased energy demand required to propel a wheelchair with a flat tyre.

Solid non-pneumatic tyres, fully eliminate the risk of puncture or the need for frequent pressure maintenance. However, they tend to be heavier and less comfortable than pneumatic tyres[2,9]. Furthermore, literature studies have found them to have higher rolling resistance than pneumatic tyres[2,10,11].

Flexible-spoke non-pneumatic tyre (FS-NPT) technology could help address these problems. However, to the authors' knowledge, this technology has never before been used in wheelchairs. FS-NPT performance is based on the properties of flexible structures (spokes) which can deform to absorb impact loads and return to their original shape upon unloading. An FS-NPT comprises a layer of deformable spokes, which are usually made of a polymeric flexible material, a thin rubber tread to provide sufficient traction, and a steel outer-ring sandwiched between the spokes and tread which maintains the circular shape of the tyre (Fig. 1a). A wide range

[1]Centre for Biomechanics and Rehabilitation Technologies, Staffordshire University, Stoke-On-Trent, UK. [2]School of Science and Engineering, University of Dundee, Nethergate, Dundee DD1 4HN, Scotland. [3]Warwick Manufacturing Group, University of Warwick, Coventry, UK. ✉email: pchatzistergos@gmail.com

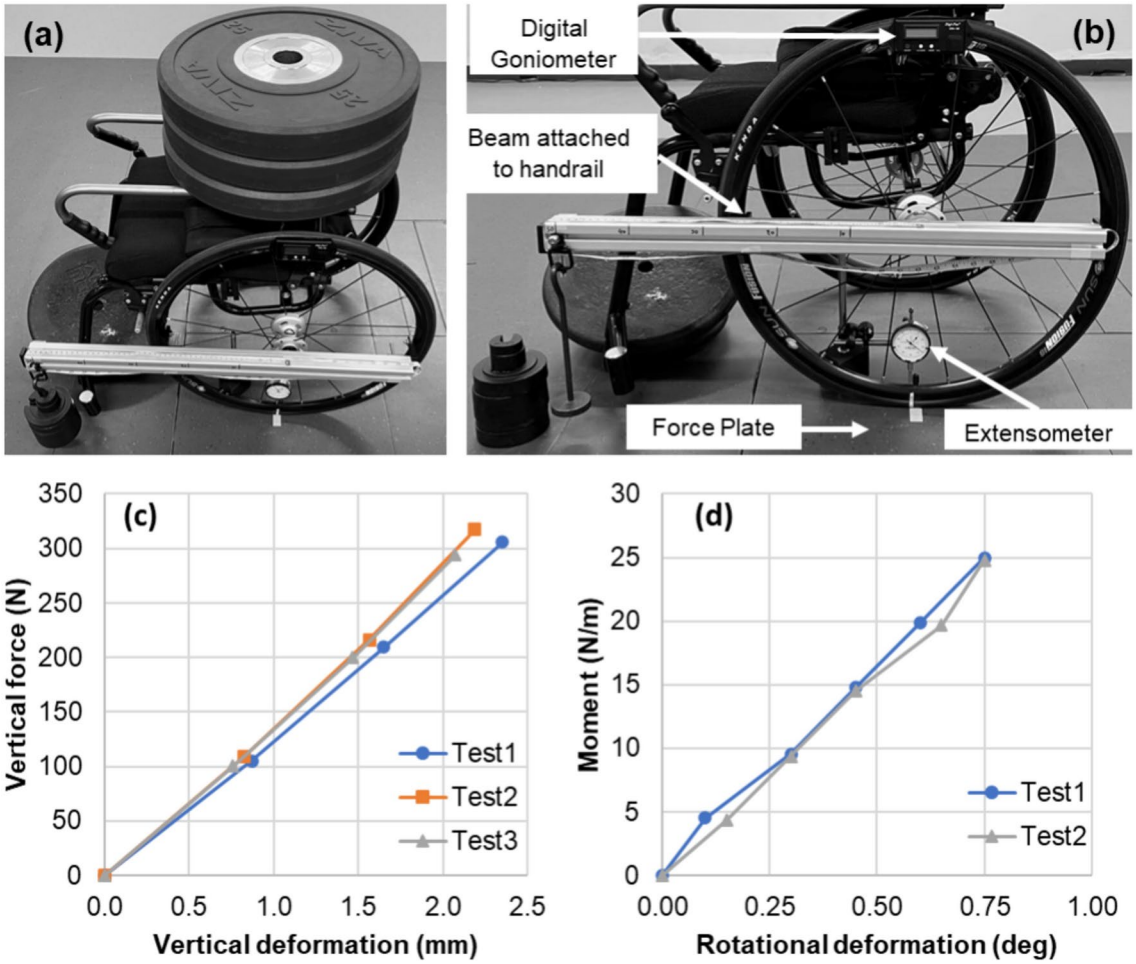

Fig. 1. The testing set-up for the measurement of vertical and rotational stiffness of a commercially available pneumatic wheelchair tyre (**a**,**b**). Vertical force—deformation (**c**) and moment—rotation graphs (**d**) for individual test repetitions.

of different spoke designs have been proposed in the literature with honeycomb structures being among the most commonly used[12–14].

To date, FS-NPTs have been used in automotive, aerospace, military, and recreational applications where they have been proven to be durable and capable of offering high levels of comfort and propulsion efficiency[15,16]. At the same time, the disadvantages of FS-NPTs identified so far do not seem relevant to wheelchair applications. More specifically, relevant literature indicates that the key limitation of FS-NPTs is their tendency to excessively vibrate and overheat at high speeds[14]. This can be a significant limitation for automotive or other high-speed applications but does not affect their applicability in relatively low-speed applications such as wheelchairs.

Another advantage of FS-NPTs is their unique capacity to fine-tune their mechanical characteristics by modifying the geometry of their spokes[12]. This feature of FS-NPT technology has been used to optimise tyre design for different applications. In the case of wheelchairs, this inherent characteristic of FS-NPTs can open the way to unique possibilities to optimise a tyre's mechanical characteristics to the body mass and specific needs of individual users.

Mechanical tuning can include adapting the tyre's vertical and rotational stiffness for optimal performance. Unlike current tyre technology, FS-NPTs possess the ability to decouple vertical from rotational stiffnesses to allow advanced tuning[15]. The vertical (or radial) stiffness of a tyre quantifies the vertical force needed to generate a set amount of vertical deformation and influences user comfort[17]. A tyre with relatively lower vertical stiffness is more likely to be capable of offering better suspension properties than a stiffer tyre leading to increased dampening of impact loads and vibrations to provide a more comfortable ride[9]. At the same time, a softer tyre is also likely to have greater resistance to rolling leading to poorer wheeling efficiency[5,7].

The tyre's rotational stiffness can be quantified as the rotational moment applied to the wheel divided by the produced rotation (Nm/deg) and is linked to wheeling efficiency. In the literature, this has been also referred to as the longitudinal or circumferential stiffness. A tyre with high rotational stiffness will have lower energy losses caused by tyre deformation and should therefore be easier for a user to propel. Increased rotational stiffness has been linked to reduced rolling resistance and better braking efficiency[15,17].

Considering the inherent advantages of FS-NPTs over existing relevant tyre technologies, one can hypothesise that FS-NPTs are likely to be a good candidate technology for wheelchairs (i.e. puncture proof, no need for pressure maintenance, capacity for subject-specific optimisation of comfort and wheeling efficiency). However, their suitability for this specific application has not been explored in the literature as of yet.

As a first step, this study aims to test whether FS-NPT technology can replicate the mechanical characteristics of conventional pneumatic wheelchair tyres. To meet this aim, the vertical and rotational stiffness of a typical, commercially available pneumatic tyre was measured first to provide the baseline characteristics for assessing the potential effectiveness of FS-NPTs. A validated Finite Element (FE) model of a honeycomb spoke was used to design a parametric model of a complete wheelchair FS-NPT. This model was used to quantify the effect of different design parameters and their interaction on tyre characteristics and to explore the capacity of FS-NPTs for tuning. Utilising this tuning, the end goal was to produce a tyre that has: (a) the same vertical stiffness as the baseline pneumatic tyre, (b) similar or greater rotational stiffness and (c) similar or lower mass than the baseline pneumatic tyre.

Pneumatic tyres were used as a benchmark because of their apparent superior performance relative to solid non-pneumatic tyres regarding comfort and wheeling efficiency[2,10,11]. Also, to maximise the potential relevance of results, the wheelchair FS-NPT was designed to be mounted on existing conventional wheelchair wheels.

Results

Baseline characteristics of a typical pneumatic tyre

A typical active wheelchair frame (RGK Hi-Lite) with standard pneumatic tyres (Kenda Koncept, 23-540, 24 × 1) was used. The total mass of the tyre and of its inner tube was 0.408 kg.

Vertical stiffness was measured by incrementally increasing loading on the wheelchair using calibrated weights to the average weight of a wheelchair user[18]. For each increment of loading, tyre deformation was measured using an extensometer positioned on the inner wheel rim directly above the contact region (Fig. 1a, b). A built-in ground force plate recorded the vertical reaction force as a result of the applied load. The average of the maximum applied vertical force measured by the load plate was equal to 306N ± 12N and it resulted in a maximum vertical deformation of 2.20 mm ± 0.14 mm. Equivalent stiffness was calculated by dividing maximum force over maximum deformation and it was equal to 139kN/m ± 8kN/m (Fig. 1c).

Rotational stiffness was measured by first applying a vertical load simulating the weight of an average wheelchair user before incrementally increasing the rotational moment on the wheel's hub using suspended weights (Fig. 1a, b). A goniometer was used to measure the respective rotational deformation of the tyre for each increment of moment. The maximum applied moment was equal to 24.8Nm ± 0.1Nm which corresponds to the moment generated by a user during an initial wheeling stroke on a level surface[19]. Maximum deformation was 0.75 deg ± 0.05 deg. Equivalent rotational stiffness was calculated by dividing maximum moment over maximum rotation and it was equal to 33.2Nm/deg ± 0.2Nm/deg (Fig. 1d).

Design of an FS-NPT

A parametric FE model of an FS-NPT that can be fitted on the same wheel as the baseline pneumatic tyre was designed using a honeycomb spoke structure (Fig. 2a). The honeycomb spokes were enclosed between two thin strips made from the same material to produce a continuous spoke layer. A stainless-steel outer ring and rubber tread were added as separate thin layers to complete the design of the FS-NPT (Fig. 2b). Following a mesh convergence analysis it was concluded that ≈ 840,000 elements were needed to ensure independence of results from the mesh density.

The honeycomb spokes were assumed to be made from a 3D-printable thermoplastic polyurethane (TPU95A). The mechanical properties of TPU95A were experimentally measured. This specific material was chosen to support preliminary prototyping and the validation of spoke FE models. More specifically, a comparison against experimental results indicated that the FE models were able to predict the mechanical behaviour of the honeycomb spokes with an error of 3%, which was deemed acceptable[20].

According to relevant literature, the specific design parameters that define the mechanical behaviour of a honeycomb FS-NPT are: the thickness of the plates of the spoke (PT), the width of a spoke (W), the internal angle measured between the non-horizontal plates and the vertical axis (A), spoke count (S) and the thickness of the stainless steel outer ring (RT)[12] (Fig. 2b). The minimum and maximum value for each design parameter was decided based on preliminary testing to avoid overlap and to ensure manufacturability[20]. All other parameters were adapted to ensure that the simulated FS-NPT fits on the wheel that was used for baseline testing without changing the total height of the wheelchair (Fig. 2c).

For this geometrical configuration, a closed form equation was developed to calculate the total mass of the FS-NPT based on the total volume of individual components and their assumed material density. Starting from an initial design where all modifiable design parameters had their minimum value, each parameter was gradually increased to its maximum and the effect on mass was calculated (Fig. 2d). Only one parameter was changed at each given time. It was found that outer ring thickness had the strongest effect on mass, followed by spoke plate thickness and spoke count. In these cases, going from the minimum to the maximum value increased mass by 0.168 kg, 0.077 kg, and 0.020 kg respectively. The effect of the remaining two parameters on the tyre's mass was significantly smaller. Indeed, increasing spoke angle or width from their minimum to their maximum values increased the mass of the FS-NPT only by ten or four grams respectively (Fig. 2d).

When compared against the baseline mass of a conventional pneumatic wheelchair tyre, it appears that values close to their minimum are likely to be needed for the outer ring and spoke plate thickness to produce an FS-NPT that is not heavier than the baseline (Fig. 2d).

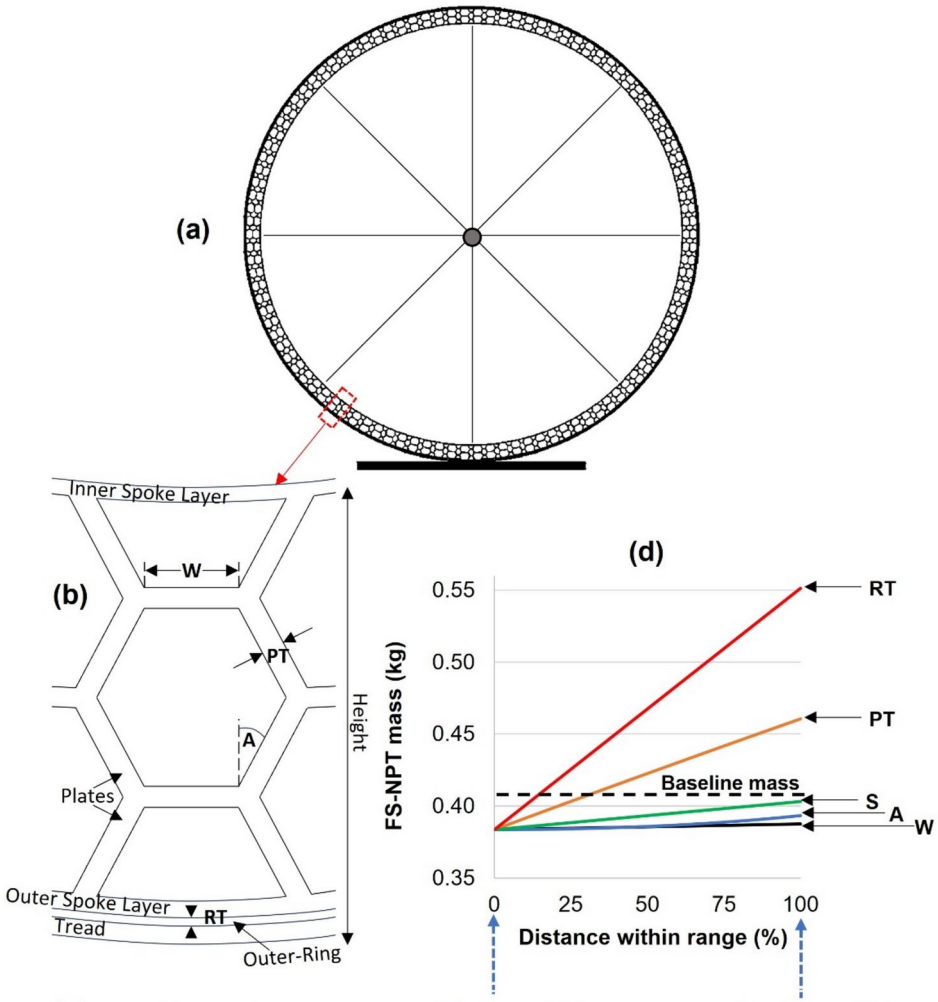

(c)

Parameter	Minimum Value	Maximum Value
Plate Thickness (PT)	1.25mm	2mm
Width (W)	3mm	4.5mm
Angle (A)	15°	39°
Spoke Count (S)	90	110
Ring Thickness (RT)	0.25mm	1mm

Fig. 2. Schematic representation of the wheelchair FS-NPT (**a**) with a detailed description of the design parameters of the honeycomb spoke (**b**). The acceptable range of each design parameter is shown (**c**) together with their effect on tyre mass (**d**). The effect on mass is plotted for increasing design values from 0 to 100% of their accepted range. The baseline mass of the tested pneumatic tyre is also shown for reference.

FS-NPT mechanical behaviour

An initial round of virtual experimentation was done to get an overview of the mechanical behaviour of the FS-NPT. To this end, the Taguchi robust design of experiments method was used to objectively select the values of the design parameters for these simulations. The Taguchi method was used because it enables the design of experiments that highlight the effect of individual parameters as well as their interaction with the minimum possible number of simulations.

Sixteen different scenarios covering the entire range of acceptable values were tested (Table 1). To this end, the previously developed FE model was used to simulate the loading scenarios of baseline testing (Fig. 3a) and to estimate the vertical and rotational stiffness of the FS-NPT. Peak von-Mises stress in the spokes was also extracted.

Results indicated that the designed FS-NPTs can have vertical stiffness that is comparable to the baseline pneumatic tyre (Fig. 3b). Indeed, equivalent vertical stiffness ranged between 92kN/m and 340kN/m (Table 1). However, in contrast to baseline testing, vertical deformation did not necessarily increase linearly with loading in all cases (Fig. 3c). This was due to buckling in the spokes closest to the ground in two cases (designs 1 and 2).

Design	Input parameters					Stiffness		Stress (MPa)	Mass (kg)
	PT (mm)	W (mm)	A (deg)	S	RT (mm)	Vertical (kN/m)	Rotational (Nm/deg)		
1*	1.25	3.0	15	90	0.25	95	392	37.2	0.380
2*	1.25	3.5	23	97	0.50	92	608	29.0	0.445
3	1.25	4.0	31	103	0.75	131	674	22.8	0.512
4	1.25	4.5	39	110	1.00	131	749	15.2	0.583
5	1.50	3.0	23	103	1.00	259	786	12.3	0.590
6	1.50	3.5	15	110	0.75	294	781	11.4	0.542
7	1.50	4.0	39	90	0.50	116	822	22.8	0.476
8	1.50	4.5	31	97	0.25	153	789	19.7	0.423
9	1.75	3.0	31	110	0.50	226	1250	17.1	0.520
10	1.75	3.5	39	103	0.25	165	1179	17.1	0.464
11	1.75	4.0	15	97	1.00	340	806	9.6	0.612
12	1.75	4.5	23	90	0.75	240	877	14.8	0.549
13	2.00	3.0	39	97	0.75	203	1309	17.6	0.594
14	2.00	3.5	31	90	1.00	257	1042	15.9	0.632
15	2.00	4.0	23	110	0.25	297	1244	12.5	0.492
16	2.00	4.5	15	103	0.50	339	1106	10.3	0.537

Table 1. The 16 initial design scenarios produced using the Taguchi robust design of experiment method and respective computational results. These include the equivalent vertical and rotational stiffness and the peak Von Mises stress in the spokes. The total tyre mass of each design is also shown. Designs 1 and 2 are indicated as the two only scenarios where buckling was observed (*). *Scenario where buckling was observed.

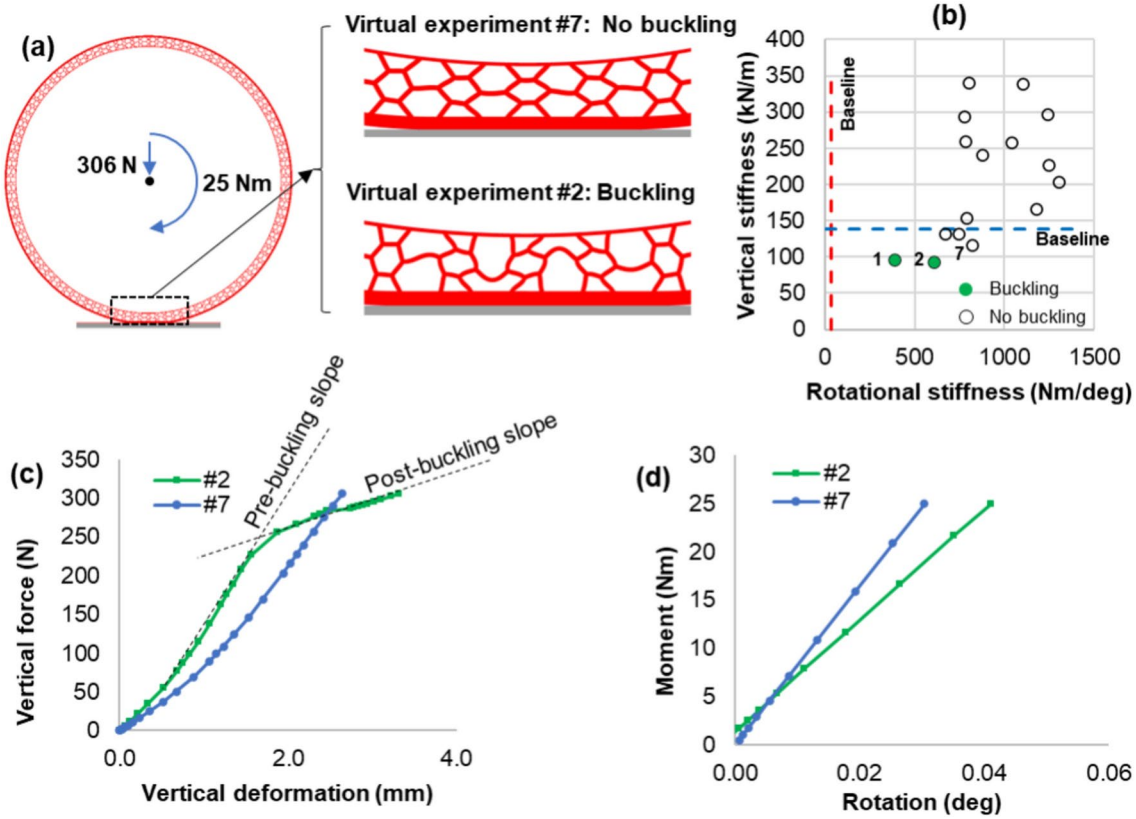

Fig. 3. (**a**) Schematic of the loading scenarios applied to the models and the deformed shapes of a model that buckled (design 2) and one that didn't buckle (design 7). (**b**) Graph overview of the vertical and rotational stiffness that was achieved by the designs of Table 1. Baseline vertical and rotational stiffness is shown for reference. Buckled designs 1 and 2 are highlighted in green. The softest of the designs that did not buckle (design 7) is also indicated on the graph. (**c**) Comparison between the force—displacement behaviour of designs 2 and 7. The pre/post-buckling slopes of the graph for design 2 are also indicated. (**d**) Comparison between the moment—rotation graphs of designs 2 and 7.

The two cases where buckling occurred exhibited the largest vertical displacement and lowest equivalent stiffness out of the 16 designs tested here (Fig. 3b).

Buckling had a clear effect on the deformed shape of the spokes (Fig. 3a) and on the vertical load—vertical displacement graph. Buckled designs exhibited a relatively high pre-buckling stiffness followed by significantly reduced stiffness after buckling. Indicatively, the slope of the force deformation graph in design 2 changed from 173kN/m pre-buckling to 50kN/m immediately after buckling (Fig. 3c). The respective change for design 1 was from 216kN/m to 11kN/m. This unique capability to become significantly softer after a threshold of vertical load can potentially be very useful to enable tuning the stiffness of tyres differently for different loading scenarios (e.g. stiff during rolling but soft during pavement dismount). However, the buckling threshold in the cases studied here was relatively low. Indeed, buckling was initiated for vertical loads of around 220N (Fig. 3c). This buckling threshold is low enough to mean that simply sitting on the wheelchair would lead to buckling rendering these tyres inadequately stiff for the intended use.

When a rotational moment of 25Nm was also imposed to the models, the FS-NPTs exhibited levels of stiffness that were significantly higher than the baseline pneumatic tyre (Fig. 3b). Indeed, the measured maximum rotations ranged between 0.02 deg to 0.06 deg resulting in rotational stiffness ranging between 392 Nm/deg and 1309Nm/deg respectively (Table 1). In this case rotation increased linearly with moment for all simulated scenarios (Fig. 3d).

Peak stresses in the spokes ranged between 9.6 MPa and 37.2 MPa with the two buckled designs exhibiting the highest values (Table 1). Peak stress for the designs that did not buckle reached a maximum value of 22.8 MPa. To place these values in context, the reported ultimate stress of TPU95A is 24 MPa[21]. Even though the observed stresses were relatively lower, these results highlight the risk of designing an FS-NPT that is not strong enough to provide the needed durability.

The effect of different design parameters on FS-NPT mechanical characteristics

Linear regression analysis was used to quantify the effect of individual design parameters on vertical and rotational stiffness. To ensure that an adequate number of data points was included, the same regression analysis was repeated for increasing sample size until the values of the regression coefficients stabilised (Fig. 4a). FS-NPT designs where buckling was observed were excluded.

Starting from 14 scenarios (designs 1 and 2 were excluded due to buckling), sample size was increased in increments of ten. To this end, the previously developed FE model was used to estimate the vertical stiffness, rotational stiffness and peak spoke stress for random FS-NPT designs. These additional designs were produced using a random number generator which assigned values to individual design parameters within the previously identified limits of acceptable values (Fig. 2c). It was concluded that the regression coefficients stabilised to a satisfactory degree for a total sample size of 74 (Fig. 4a). Indicatively, for this sample size the average % change relative to the previous increment was 2.1% (±3.4%), 1.9% (±2.0%) and 3.9% (±2.4%) for vertical stiffness, rotational stiffness and spoke stress respectively. A table with all 74 scenarios and respective results can be seen in Supplementary data 1.

This final regression model indicated that plate thickness, angle, spoke count and ring thickness had a significant effect on vertical stiffness, rotational stiffness and spoke stress. Spoke width had a significant effect only on rotational stiffness (Fig. 4b–d).

To put the observed effects in perspective, changes in vertical and rotational stiffness are presented as % of the vertical and rotational stiffness of the baseline pneumatic tyre respectively. Changes in maximum spoke stress are presented as % of the ultimate stress of TPU95A[21].

Increasing plate thickness and spoke count has a clear strengthening effect on the tyre evidenced by increased vertical stiffness, increased rotational stiffness, and reduced spoke stresses. Increasing plate thickness by 10% of its acceptable range (i.e. 0.075 mm) increases vertical and rotational stiffness by 8.7% (12.1 kN/m) and 172.3% (57.2 Nm/deg) respectively and reduces spoke stress by 1.9% (463 kPa). An equivalent change in spoke count (i.e. 2 spokes) increases vertical stiffness by 2.8% (3.9 kN/m), rotational stiffness by 55% (18.3 Nm/deg) and reduces stresses by 1.6% (388 kPa) (Fig. 4b-d).

Based on the above, plate thickness appears to have a stronger effect on stiffness and stress than spoke count. However, when tyre mass is also considered (Fig. 2d), increasing spoke count seems to be the most efficient way to strengthen the tyre. It is calculated that for every one gram of mass added to the tyre due to increased plate thickness, vertical stiffness increases by 1.6kN/m, rotational stiffness increases by 7.3Nm/deg and peak stress in the spokes reduces by 59 kPa. The same increase in mass due to increased spoke count increases vertical stiffness by 2.0kN/m, rotational stiffness by 9.4Nm/deg and reduces peak stresses in the spokes by 200 kPa.

Increasing ring thickness makes the tyre stiffer in compression but more deformable in rotation. In this case, an increase by 10% of the acceptable range (i.e. 0.075 mm) leads to 3.2% (4.4kN/m) increase in vertical stiffness and 28.5% (9.5 Nm/deg) reduction in rotational stiffness (Fig. 4b, c). It also leads to a reduction in peak stresses by 1.0% (241 kPa) (Fig. 4d). When mass is also taken into account, it can be concluded that ring thickness is a relatively inefficient way to increase vertical stiffness or to reduce stresses (Fig. 2d). In this case, for every one gram of added mass due to increased ring thickness, vertical stiffness increases only by 0.3kN/m and spoke stress decreases only by 14 kPa.

Angle is the only design parameter that can significantly change the mechanical characteristics of the tyre without significantly changing its mass (Fig. 2d). Increasing angle by 10% of the acceptable range (i.e. 2.4 deg) reduces vertical stiffness by 9.8% (13.6 kN/m), increases rotational stiffness by 71.4% (23.7 Nm/deg) and spoke stresses by 3% (744 kPa) (Fig. 4b,c). In cases where relatively reduced rotational stiffness is an accepted trade-off, reducing angle to produce a design closer to a rectangular shape can be a very effective strategy to stiffen and strengthen the tyre in compression.

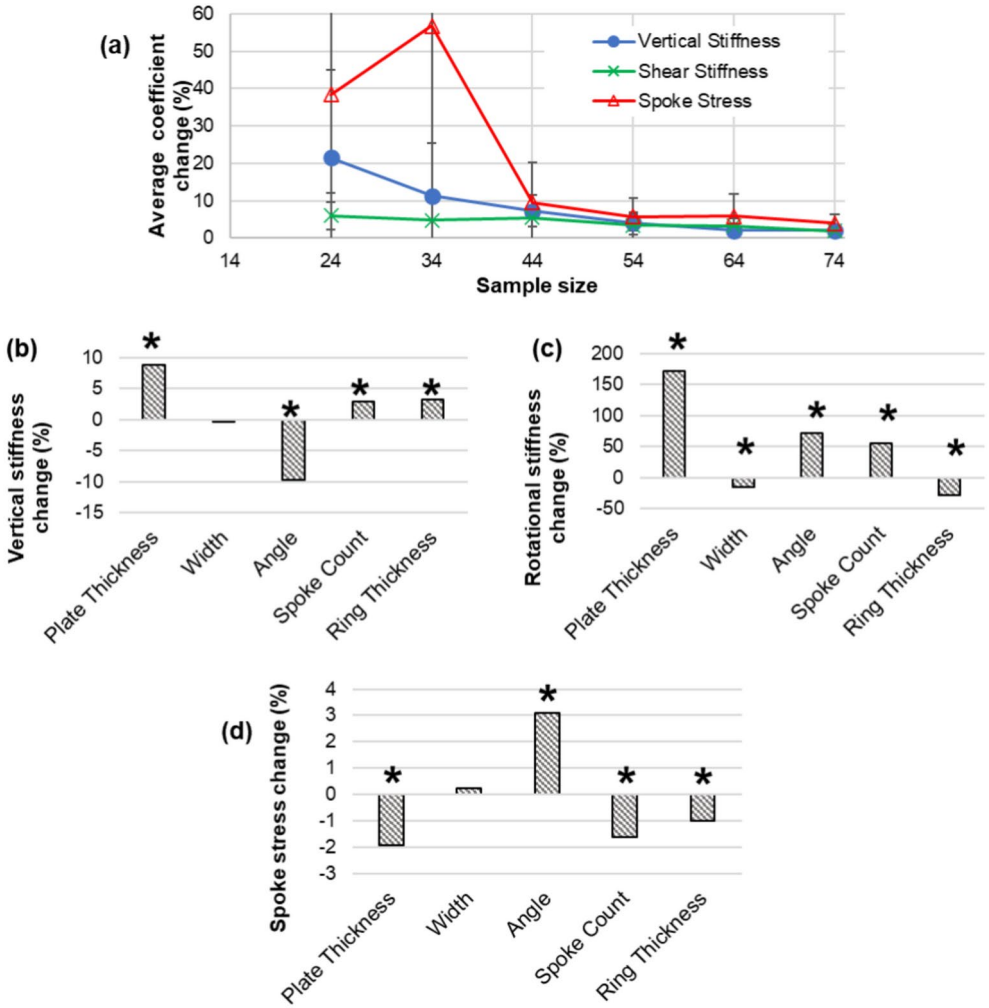

Fig. 4. (**a**) The average change in multiple linear regression coefficients with increasing sample size. In this case, % difference is calculated relative to the previous iteration. (**b**–**d**) Calculations according to the final regression model (sample size 74) on the effect of individual design parameters on vertical stiffness (**b**), rotational stiffness (**c**) and peak spoke stress (**d**). Change in mechanical characteristics is calculated for an increase in each design parameter equal to 10% of its respective acceptable range (assumed increase - plate thickness: 0.075 mm, spoke width: 0.15 mm, spoke angle: 2.4 deg, spoke count: 2, ring thickness: 0.075 mm). To put the observed effects into perspective, changes in vertical and rotational stiffness are presented as % of the vertical (139 kN/m) and rotational (33.2 Nm/deg) stiffness of the baseline pneumatic tyre respectively. Changes in maximum spoke stress are presented as % of the ultimate stress of TPU95A (24 MPa)[21]. Statistically significant effects are indicated with *.

Lastly, spoke width appears to be the least influential design parameter tested. In this case increasing its value by 10% of the acceptable range (i.e. 0.15 mm) leads only to a relatively modest reduction of 15% (5Nm/deg) in rotational stiffness (Fig. 4c). Spoke width did not appear to have a significant effect on vertical stiffness or spoke stress.

FS-NPT design tuning

The previous results were used to develop a tuning process to produce an FS-NPT that mimics the vertical stiffness of the baseline pneumatic tyre while achieving higher rotational stiffness and lower mass.

Considering the effect of individual parameters, plate thickness, ring thickness and spoke width were set to their minimum acceptable values (i.e. 1.25, 0.25 and 3 mm respectively). Starting from its maximum value, spoke count was used as an initial tuning parameter followed by angle which was used for fine-tuning.

Further virtual experimentation indicated that maximum spoke count (i.e. 110) produces vertical stiffness equal to 210kN/m. As expected, vertical stiffness reduced linearly with reducing spoke count. This reduction was linear until a value of 106 spokes (Fig. 5a). Further reduction led to increasingly larger changes in vertical stiffness due to buckling. Based on this, it was decided that 106 was the minimum acceptable spoke count. Minimising spoke count was deemed important to minimise tyre mass. Vertical stiffness for this design was 198kN/m (Fig. 5a).

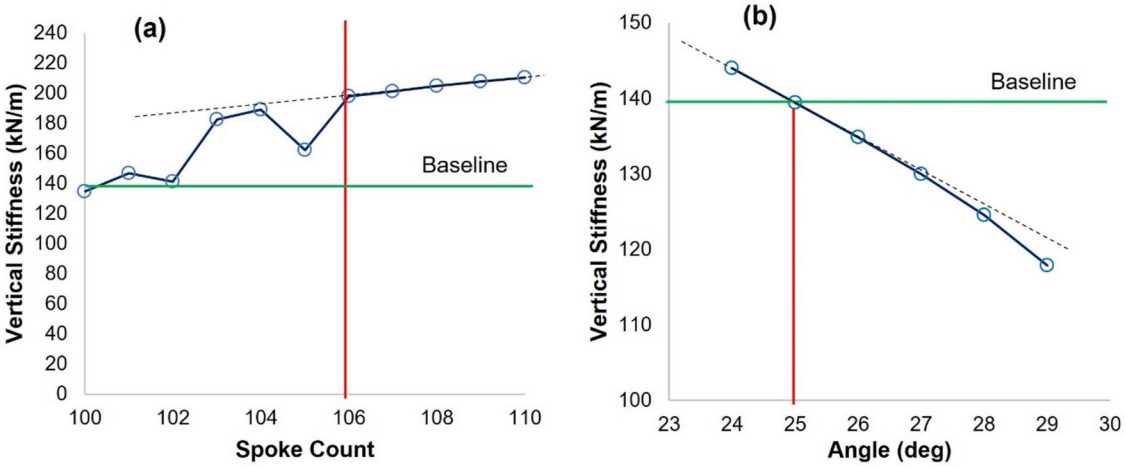

Fig. 5. Virtual experimentation results to identify the spoke count (**a**) and angle (**b**) for a FS-NPT with the same vertical stiffness as the baseline pneumatic tyre. The selected values and baseline stiffness are indicated in the graphs.

For these previous simulations, angle was kept to its minimum value (i.e. 15 deg). Angle was then used as the final fine-tuning parameter to reduce vertical stiffness to the target of 139kN/m. To reduce the number of virtual experiments, the multiple regression equation on the effect of the five design parameters on vertical stiffness was used to produce an initial estimation of the needed angle value. Based on this, a final set of simulations was done for angle values ranging between 29 and 24 deg. It was concluded that an angle of 25 deg replicates the vertical stiffness of the baseline pneumatic tyre (Fig. 5b).

The final FS-NPT design that was produced through this fine-tuning process had a plate thickness of 1.25 mm, spoke width equal to 3 mm, a 25 deg angle, 106 spokes and a ring thickness of 0.25 mm (Fig. 6a,b). This design did not buckle under the externally applied load, and it achieved a vertical stiffness equal to 139kN/m. Its rotational stiffness was 665Nm/deg and its mass was equal to 0.401 kg. Peak stress in the spokes was 19.4 MPa (Fig. 6c).

Discussion

The results presented here indicate that it is feasible for a wheelchair FS-NPT to replicate the vertical stiffness of a typical wheelchair pneumatic tyre while at the same time achieving higher rotational stiffness and reduced mass. To maximise the potential relevance of results, this first-ever wheelchair FS-NPT was designed to be mounted on a wheelchair without the need for major modifications to existing conventional wheels.

Equally important, this study also demonstrates that the mechanical characteristics of a wheelchair FS-NPT can be easily tuned to specific, relevant targeted values. Following a series of virtual experiments, it was found that, for the honeycomb spoke design studied here, spoke count and angle are likely to be the two most effective tuning parameters. Indeed, increasing spoke count achieved the greatest increase in stiffness (vertical and rotational) and greatest reduction in stresses for each gram added to the tyre's mass. Reducing the spoke angle also significantly increased vertical stiffness, but in this case, this was also accompanied by a significant reduction in shear stiffness. Considering that its effect on tyre mass is relatively small highlights angle as a useful parameter for fine-tuning. Increasing plate and ring thickness can also significantly strengthen the tyre but this is also accompanied by a significant increase in mass. Using the minimum possible thickness values appears to be the best strategy for design optimisation.

Keeping mass as low as possible is important for the relevance and potential applicability of FS-NPTs in wheelchairs. This is because a heavy tyre will require more energy to overcome inertia and increase rolling resistance[22]. Moreover, a heavier tyre will make it more difficult for independent manual wheelchair users to dismantle and transport their wheelchairs (e.g. when getting into/out of their car).

In this study, FS-NPT design was tuned with the help of a large number of virtual experiments. Developing a design optimisation method that does not require use of FE modelling would significantly enhance the applicability and potential impact of this technology. A glimpse of a potential solution is given in this study, where a regression model was used to narrow down the range of angle values that can achieve the target vertical stiffness (Fig. 5b). In this case, a final set of FE analyses was still needed, but the number of simulations were significantly reduced. Further research will be needed to explore whether statistical modelling is likely to achieve satisfactory accuracy to completely replace the need for FE modelling for the optimisation of FS-NPT characteristics[23].

The vertical stiffness of a wheelchair tyre is crucial for cushioning and comfort. From other rehabilitation engineering applications, it can be assumed that an optimum tyre stiffness is likely to exist[24]. Optimum stiffness could depend on the intensity of daily loading and the user's body mass[25], but current literature on wheelchair technology does not enable inferring its value. To account for this fact, the present study aimed to tune the mechanical behaviour of the proposed FS-NPT to match the vertical stiffness of a conventional commonly used

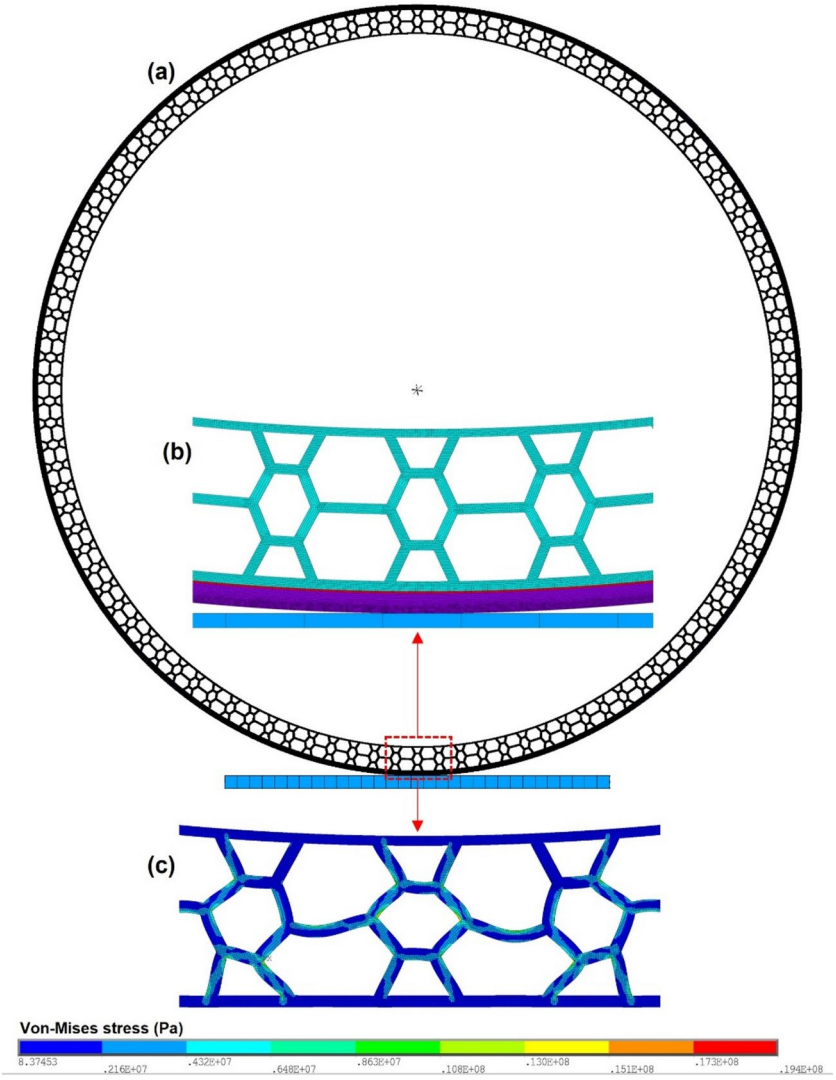

Fig. 6. The final FS-NPT design (**a**,**b**) and the distribution of von-Mises stresses in the most heavily loaded spokes (**c**). For better presentation of stresses, the outer ring and tread are excluded from the contour plot.

pneumatic tyre. In doing so, this study demonstrates that FS-NPTs can achieve a vertical stiffness that is relevant to the specific application. Further research will be needed to explore how this unique capability for tuning vertical stiffness can be best utilised to achieve optimum comfort.

Among the unique possibilities of wheelchair FS-NPTs revealed in this study was also the potential to design tyres that exhibit different levels of vertical stiffness for different magnitudes of external load. More specifically, when compressive loading on the spokes exceeds a critical threshold, buckling of the spokes occurs which leads to substantial softening (Fig. 3a). This unique characteristic means that it is feasible to design a wheelchair tyre that is relatively stiff when loaded with vertical forces similar to the user's body weight but becomes significantly softer when vertical loading is significantly increased and there is need for more cushioning. Scenarios where cushioning is very important include pavement dismount or rolling over a cleat/bump. In the first case, buckling helps the tyre to deform and to absorb more energy than what it would otherwise be able to absorb. In the latter case, buckling means that the tyre can deform around the cleat/bump to reduce the vertical displacement of the wheel axis for smoother rolling. This possibility of FS-NPTs to adapt their stiffness to the demands of different loading scenarios could enable combining maximum wheeling efficiency with maximum shock absorption and optimum cushioning.

In the virtual experiments conducted here, buckling was observed for loads that were too low to enable utilising this unique feature. However, buckling is an inherent characteristic of the tested structures that takes place after a critical threshold has been exceeded[26]. Similar to stiffness, the buckling threshold is likely to be tuneable[26]. In this study spoke number and angle were used during the final stages of design tuning to ensure that the targeted vertical stiffness was achieved while the buckling threshold remained above the applied vertical force. Further research is needed to identify the optimum way of controlling and tuning the buckling threshold of the spokes of FS-NPTs.

Comfort, wheeling efficiency, and reduced mass were considered key desirable characteristics for wheelchair tyres. Even though this assumption is supported by studies on wheelchair user needs[1,27,28], literature on what wheelchair users desire specifically from their tyres is scarce. Addressing this gap in knowledge is important to support future research to personalise/optimise FS-NPTs.

Relevant literature indicates that a higher rotational stiffness can be linked to reduced rolling resistance and thus improved wheeling efficiency[15]. Virtual experimentation indicated that FS-NPTs are likely to be substantially stiffer than pneumatic tyres in rotation. Although, this is clearly a positive result, its validity will have to be further explored and confirmed. In the FE models tested here, the FS-NPT was assumed to be perfectly bonded to the wheel which might have led to an overestimation of rotational stiffness. The level of relative sliding between the FS-NPT and the wheelchair wheel will depend on the effectiveness of the mounting mechanism that will be used.

Similar to existing solid non-pneumatic tyres, FS-NPTs could also reduce the risk of being stranded (e.g. due to a puncture) and reduce the maintenance burden on users (no need for pressure maintenance). However, for these benefits to be realised, the produced FS-NPTs will have to be robust and durable enough to sustain the loading of everyday use without being damaged. This study offers an initial indirect assessment of the potential durability of FS-NPTs based on the magnitudes of the observed stresses. Additionally, the results presented here indicate that stresses in the spokes during wheeling on a flat surface are likely to be lower than the ultimate stress for TPU95A. A combination of lab-based cyclic and real-world testing will be needed to ensure that the produced FS-NPTs are durable and robust enough to sustain repetitive loading of significantly higher magnitudes than the ones simulated here. It is important to highlight that being more durable does not refer only to avoiding catastrophic failure but also to having a tyre that can maintain its desired mechanical properties for longer (e.g. does not become significantly softer over time). The selection of appropriate materials and manufacturing methods will be critical to this end.

In this study, FS-NPT spokes were assumed to be made from TPU95A. This 3D-printing material was used to support preliminary prototyping and the validation of FE spoke models. Materials already used in automotive applications of FS-NPTs appear to be ideal candidates to be explored during future work. These materials are significantly stiffer and stronger than the TPU95A used here. Transitioning to such materials could maximise the chances of developing a durable and lightweight wheelchair FS-NPT[15,29].

Methods

Measurement of baseline vertical and rotational stiffness

Baseline values of vertical and rotational stiffness were measured for a standard commercially available pneumatic tyre (Kenda Koncept, 23-540, 24 × 1). The tyre was inflated to a pressure of 80 psi/552 kPa as per the manufacturer's guidelines and was mounted to a typical active wheelchair frame (RGK Hi-Lite, max load of 125 kg). All tests were repeated at least twice to ensure there was minimal variability.

Prior to testing, the front wheels (caster wheels) of the wheelchair were removed, and weights were added to the footplates to ensure the wheelchair would not move or slide during testing (Fig. 1a). One wheelchair tyre was positioned on top of a force plate (AMTI OPT464508HF AMTI, USA; sampling rate 1000 Hz) capable of measuring vertical and parallel to the ground reaction forces.

For the measurement of vertical stiffness, an extensometer (LINEAR, 0.01 mm resolution) was placed on the rim of the wheel just above the contact region to measure the vertical deformation of the tyre (Fig. 1a, b). Vertical load on the tyres was gradually increased with the help of calibrated weights which were placed on the wheelchair seat (Fig. 1a). The total weight on the wheelchair seat was increased in increments of 245N (25 kg) to a maximum of 736N (75 kg), which corresponds to the average weight of a wheelchair user. Force plate measurements indicated that this loading process led to an average maximum force applied to the tyre of 306N ± 12N. For each increment of externally applied vertical load, the vertical reaction force applied to the tyre was measured from the force plate and the respective vertical deformation was measured from the extensometer. Equivalent stiffness was calculated by dividing maximum force over maximum deformation (Fig. 1c).

For the measurement of rotational stiffness, a metallic beam was fixed to the hub of the wheel to enable the application of rotational moments using suspended weights (Fig. 1a, b). A digital goniometer (Digi-Pas DWL-180, ± 0.05° accuracy) was also placed at the top of the tyre (on the side) which measured rotational deformation in degrees (Fig. 1a, b). Before any rotational load was applied, a total of 75 kg load was added to the wheelchair seat to simulate the weight of a user and to ensure there is enough friction between the tyre and force plate to prevent any relevant sliding. The goniometer was zeroed and rotational moment was gradually increased using suspended weights (Fig. 1a, b). The applied moment was increased to a maximum value of 25Nm by changing the distance of the suspended weights from the tyre's central hub along the metallic beam (increments of 5Nm). The maximum applied moment corresponds to average values from the literature for a user's initial wheeling stroke on a level surface[19]. The actual rotational moment applied to the wheel was calculated as the product of the generated parallel to the ground reaction force (measured by the force plate) and the distance between the tyre hub and the ground. The respective rotational deformation was measured from the digital goniometer. Equivalent rotational stiffness was calculated by dividing maximum applied moment over the resulting rotation (Fig. 1d).

Markings on the tyre and floor were used to provide a visual indication of whether there was any significant sliding during testing. To ensure no slippage had taken place, a final goniometer measurement was taken after the suspended weights were removed. In all cases the goniometer returned to zero after rotational moment was removed confirming that there was no relative sliding between the tyre and the force plate surface.

FE modelling of wheelchair FS-NPT

A 2D plane stress with thickness FE model of an FS-NPT was created assuming a honeycomb spoke structure (Fig. 3a). The design of the FE model was based on a previously validated model of individual spokes 20. The numerical analysis was carried out using Ansys Mechanical APDL 2021 R2.

The dimensions of the FS-NPT were adapted to replicate the tested pneumatic tyre (i.e. radius, height, thickness) and to ensure that the simulated FS-NPT can be mounted on the same wheel. Figure 2b shows a honeycomb spoke that would recur a number of times around the tyre. To complete the spoke layer, the honeycomb structures are enclosed between two thin layers of spoke material. An outer ring and tread are then added as separate thin layers to complete the design of the FS-NPT.

According to previous literature, the specific design parameters that can be used to tune the mechanical behaviour of a honeycomb FS-NPT are: the thickness of the plates of the spoke (PT), the width of a spoke (W), the internal angle measured between the non-horizontal plates and the vertical axis (A), spoke count (S) and the thickness of the metallic outer ring (RT)[12] (Fig. 2b). The minimum and maximum value for each factor (i.e. design parameter) was decided to avoid overlap and ensure manufacturability[20].

The total height of the honeycomb spokes and the thickness of the tread were always kept constant and equal to 18 mm and 2.5 mm respectively. To ensure that the simulated FS-NPT fits on the wheel that was used for baseline testing without changing the total height of the wheelchair, the total thickness and depth of the tyre model were always kept constant at 22 mm and 18 mm respectively.

All components were meshed using eight node plane elements (Plane183) and were designed to be bonded with each other. A total of 839,902 plane elements was used. Element size was decided based on a mesh convergence analysis.

The spokes were assumed to be made from a thermoplastic polyurethane (TPU95A) (Table 2). A set of standardised mechanical tests were conducted to calculate the mechanical properties of TPU95A (Table 2) which were then included in the FE model using a Mooney Rivlin model (Eq. 1)[30]:

$$W = C_{10}(I_1 - 3) + C_{01}(I_2 - 3) + C_{20}(I_1 - 3)^2 + C_{11}(I_1 - 3)(I_2 - 3) + C_{02}(I_2 - 3)^2 + (J - 1)^2/d, \quad (1)$$

where 'W' is the strain energy potential, 'I_1' and 'I_2' are the deviatoric strain invariants, 'C_{10}', 'C_{01}', 'C_{20}', 'C_{11}', 'C_{02}' are material coefficients characterising the deviatoric deformation of the material, 'J' is the determinant of the deformation gradient tensor, and 'd' is the compressibility parameter[20].

The outer ring and the tread were assumed to be made from stainless steel (AISI 4340), and rubber respectively (Table 2). Material properties for the rubber and stainless steel were assigned based on literature [31,32].Stainless steel was simulated as a linearly elastic material while the hyperelastic mechanical behaviour of rubber was simulated using the Ogden model (Eq. 2):

$$W(\lambda_1, \lambda_2, \lambda_3) = \sum_{i=1}^{N} \frac{\mu_i}{\alpha_i}\left(\lambda_1^{\alpha_i} + \lambda_2^{\alpha_i} + \lambda_3^{\alpha_i} - 3\right) \quad (2)$$

where 'W' is the strain energy function, 'λ' are the principle stretches, 'N' is the number of data points, and 'μ_i' and 'α_i' are the material constants[30,31].

Loading was applied in two load steps to simulate the baseline wheelchair testing. More specifically, in load-step 1, a downward vertical force was applied, subjecting the lower spokes of the tyre to compression. The magnitude of loading was equal to the average vertical ground reaction force measured during baseline testing (306 N). In load-step 2, 25 Nm of rotational moment was also applied to the model. All loads were applied at the central axis of the tyre with the help of a combination of master/slave nodes that created a perfectly rigid wheel. A frictional contact was assumed between the simulated rigid ground and the rubber tread with a coefficient of 0.7[12].

Component	Material/material model	Density (kg/m^3)	Young's modulus (GPa)	Material coefficients	Poisson's ratio
Honeycomb spokes	Thermoplastic Polyurethane (TPU95A)[20]/Money-Rivlin [Eq. 2]	1220[21]	–	C_{01} = 45.79 MPa* C_{02} = 62.58 MPa* C_{10} = −36.63 MPa* C_{11} = -58.11 MPa* C_{20} = 17.26 MPa*	0.45*
Tread	Rubber[31]/Ogden [Eq. 3]	1043[32]	–	μ_1 = 13.356 MPa α_1 = 1.633 μ_2 = −6.631 MPa α_2 = 1.9 μ_3 = 0.058 MPa α_3 = 2.456	0.49
Outer ring	AISI 4340[32]/Linearly elastic	7800[32]	210[32]	–	0.29

Table 2. Material properties for the components of the wheelchair FS-NPT used for FE simulations. Values that were experimentally calculated for this study are indicated with (*).

Virtual experiment design

The Taguchi robust design of experiment method was used to assess the effect of individual design parameters and their interaction on the tyre's mechanical characteristics. Taguchi orthogonal arrays are based on two factors: the number of independent variables (parameters) of which there are five, and the number of levels to be tested. The number of levels determines how accurate the results will be, but also increases the number of experiments required. There are previously defined Taguchi orthogonal arrays for which there is only one array which uses five parameters, and it has four levels[33] and it includes 16 experiments (Table 3). The level numbers one and four equal to the minimum and maximum values of that parameter respectively, and levels two and three would be at 33.3% and 66.7% within the range respectively. Substituting these levels into the orthogonal array gives the Taguchi design of experiments shown in Table 1.

All additional design scenarios were created using a random-number generator using the 'randbetween' function in excel. The random-number generator was set to provide random values to each and all design parameters within the previously defined accepted ranges (Fig. 2c).

Statistical analysis of results

A multiple linear regression analysis was conducted to assess the statistical significance of the effect of individual parameters. This analysis was done separately for each outcome measure as the dependent variable (vertical stiffness, rotational stiffness and spoke stress). Plate thickness, spoke width, angle, spoke count and ring thickness were used as independent variables. All statistical analyses were done using IBM SPSS Statistics.

The following conditions were confirmed before conducting any regression analysis:

- Multicollinearity (ensuring low correlations between parameters).
- Linearity (linear relationships between parameters and results).
- Homoscedasticity (ensuring dispersion of results is consistent).
- Normality of residuals (ensuring results are consistent with normal distribution histograms / normal probability plots).
- Outliers (ensuring results are within three standard deviations of the mean).
- High leverage points (ensuring leverage values are low).
- Highly influential points (ensuring Cook's distance is low).

Regression analysis was done first for the design scenarios defined using the Taguchi method. After excluding the designs that buckled (designs 1 and 2) 14 data points were included. The same analyses were then repeated for increasing sample size in increments of 10. The regression coefficients were recorded according to the following (Eq. 3):

$$\mathrm{DV} = \beta_0 + \beta_1 \mathrm{PT} + \beta_2 \mathrm{W} + \beta_3 \mathrm{A} + \beta_4 \mathrm{S} + \beta_5 \mathrm{RT} \tag{3}$$

where DV is the dependent variable, β_0 is a constant and β_1 to β_5 are the regression coefficients for plate thickness (PT), spoke width (W), spoke angle (A), spoke count (S) and ring thickness (RT) respectively.

To identify the minimum sample size needed, the change in the regression coefficients was plotted (Fig. 4a). Change was calculated as the % change relative to the previous increment.

Design No	PT	W	A	S	RT
1	1	1	1	1	1
2	1	2	2	2	2
3	1	3	3	3	3
4	1	4	4	4	4
5	2	1	2	3	4
6	2	2	1	4	3
7	2	3	4	1	2
8	2	4	3	2	1
9	3	1	3	4	2
10	3	2	4	3	1
11	3	3	1	2	4
12	3	4	2	1	3
13	4	1	4	2	3
14	4	2	3	1	4
15	4	3	2	4	1
16	4	4	1	3	2

Table 3. Taguchi orthogonal array L16b for 5 independent variables at four levels. Numbers in the parameter columns represent the level of the respective parameter from one to four.

Spoke FE model validation

Preliminary analyses and literature[12,34] illustrated that loading in the spokes of an FS-NPT is most intense for the spokes closest to the ground. To reproduce this type of loading in a laboratory setting, samples of three-spoke clusters (Fig. 7) were manufactured, and their mechanical behaviour was measured under compression loading[20]. These samples were designed to match the dimensions of a hypothetical wheelchair FS-NPT with a tyre diameter of 24 inches (0.61 m) and a total of 100 honeycomb spokes[35]. The design and dimensions of a reference honeycomb spoke were taken from literature to enable them to fit within a conventional 24-inch wheelchair wheel (Fig. 2a)[12]. The spoke features several thin plates which are interconnected to form hexagonal openings centrally and between spokes. The cluster of spokes was completed with a top and bottom support (Fig. 7a). The inner surfaces of these supports followed the arc design of the hypothetical wheel, but their outer surfaces were flat to enable testing under compression.

Honeycomb samples were produced with plate thicknesses of 1.5 mm and 2 mm while spoke height was kept constant at 18 mm. All other dimensions were also kept constant to allow assessment of thickness. The samples were manufactured via fused deposition modelling (Ultimaker S3) with a soft thermoplastic polyurethane (TPU95A).

To check that the 3D printed samples were manufactured to a high accuracy, the thickness of the plates and the depth of all samples were measured using a digital calliper. Plate thicknesses were measured for each specimen twice on each spoke and once on each connecting spoke and were averaged.

During laboratory testing, the honeycomb samples were subjected to compression (Fig. 7c) up to 50% of the specimens' height using a 10kN loading frame (Insight Electromechanical, MTS® Systems) at 2 mm/min[20]. This was to ensure that post buckling behaviour was also captured. Force and displacement values were recorded using a 10kN load cell (MTS® Systems). The acquired data was used to plot the force–displacement graphs of all samples (Fig. 7b). Five samples were printed and tested for each thickness; the results of these were averaged to improve accuracy and ensure that any random errors (e.g. imperfections in the segments from manufacturing) did not significantly influence the final results.

All honeycomb samples experienced buckling under loading leading to force–deformation graphs that had a clear peak value of force (Fig. 7b). Average (± STDEV) maximum force was 405N (± 53N) and 920N (± 34N) for 1.5 mm and 2 mm thickness respectively. For the same scenarios, the respective numerically predicted maximum forces were 391N and 920N. Using the experimental results as a reference, these results indicate a difference of 3% for the 1.5 mm thick samples and 0.5% for the 2 mm thick samples.

TPU95A material characterisation

Material characterisation of the 3D printing material (TPU95A) was also carried out to support FE modelling[20]. Dog-bone samples were designed using dimensions outlined in the standardized test method for tensile properties of plastics (ASTM D638).

The dog-bone samples were 3D printed using the same material and the same 3D printers as before. Three samples were subjected to quasi-static tensile testing (2 mm/min) using the same 10kN loading frame to record the tensile stress–strain behaviour. An optical extensometer (RTSS Videoextensometer, Limess Messtechnik & Software Gmbh) was used to measure the strain. Poisson's ratio was also calculated for one sample by rotating it

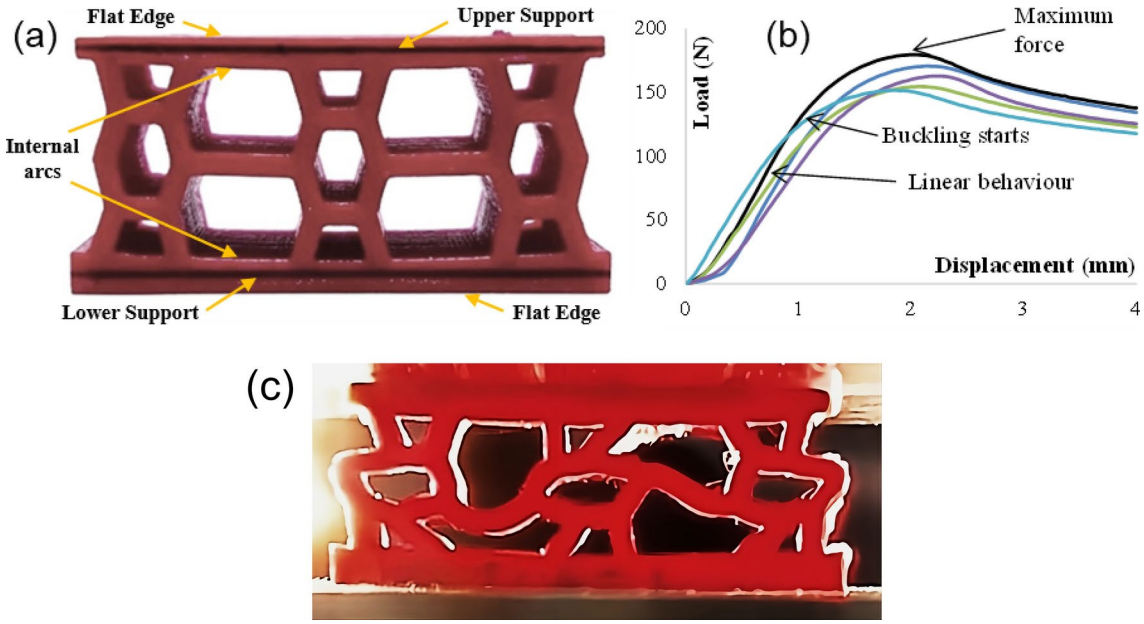

Fig. 7. (**a**) Honeycomb three spoke cluster 3D printed specimen (Ultimaker TPU95A). (**b**) Force–displacement graphs of five same-thickness samples under compression. (**c**) Specimen deformation mode under compression.

by 90° allowing measurement of lateral strain by the same extensometer. The measured stress–strain behaviour (averaged over three samples) and Poisson's ratio were combined to calculate the material's hyperplastic coefficients using the five parameter Mooney-Rivlin model [Eq. (1)][30]:

ANSYS Workbench was used to calculate the material coefficients. More specifically, the stress–strain behaviour and Poisson's ratio that were measured from the laboratory experiments were imported into ANSYS Workbench and the coefficient values that achieved the best fit of the experimental data were computed by the software's specialized tool (Table 2).

Data availability

Data is provided within the manuscript or supplementary information files.

Received: 13 August 2024; Accepted: 11 November 2024
Published online: 23 November 2024

References

1. Armstrong, W. et al. Guidelines on the Provision of Manual Wheelchairs in Less Resourced Settings. WHO Library Cataloguing-in-Publication Data (WHO Press, 2008).
2. Mclaurin, C. A. & Brubaker, C. E. Biomechanics and the wheelchair. *Prosthet. Orthot. Int.* **15**, 24–37 (1991).
3. Rodrigo, S. E. & Herrera, C. V. Chapter 11—Wheelchairs: History, Characteristics, and Technical Specifications. In *Chiral Analysis* (Elsevier, 2018).
4. Sawatzky, B. J. & Denison, I. Wheeling efficiency: The effects of varying tyre pressure with children and adolescents. *Pediatr. Rehabil.* **9**, 122–126 (2006).
5. Sawatzky, B. J., Kim, W. O. & Denison, I. The ergonomics of different tyres and tyre pressure during wheelchair propulsion. *Ergonomics* **47**, 1475–1483 (2004).
6. Gent, A. N. & Walter, J. D. Pneumatic tire. *Composites* **8**, 271 (1977).
7. Penn, N. D. et al. No more flat tyres: A trial of a tyre insert for wheelchairs. *Clin. Rehabil.* **3**, 149–150 (1989).
8. de Groot, S., Vegter, R. J. K. & van der Woude, L. H. V. Effect of wheelchair mass, tire type and tire pressure on physical strain and wheelchair propulsion technique. *Med. Eng. Phys.* **35**, 1476–1482 (2013).
9. Gordon, J., Kauzlarich, J. J. & Thacker, J. G. Tests of two new polyurethane foam wheelchair tires. *J. Rehabil. Res. Dev.* **26**, 33–46 (1989).
10. Kwarciak, A. M., Yarossi, M., Ramanujam, A., Dyson-Hudson, T. A. & Sisto, S. A. Evaluation of wheelchair tire rolling resistance using dynamometer-based coast-down tests. *J. Rehabil. Res. Dev.* **46**, 931–938 (2009).
11. Ott, J., Wilson-Jene, H., Koontz, A. & Pearlman, J. Evaluation of rolling resistance in manual wheelchair wheels and casters using drum-based testing. *Disabil. Rehabil. Assist. Technol.* **17**, 719–730 (2022).
12. Ganniari-Papageorgiou, E., Chatzistergos, P. & Wang, X. The influence of the honeycomb design parameters on the mechanical behavior of non-pneumatic tires. *Int. J. Appl. Mech.* **12**, 2050024 (2020).
13. Mohan, A., Johny, C. A., Tamilarasu, A., Bhasker, J. P. & Ravi, K. Design and analysis of non-pneumatic tyre. IOP Conf. Ser. Mater. Sci. Eng. 263, (2017).
14. Umesh, G. C. & Amith Kumar, S. N. Design and analysis of non-pneumatic tyre (NPT) with honeycomb spokes structure. *Int. J. Eng. Sci. Comput.* **6**, 2136–2140 (2016).
15. Deng, Y., Wang, Z., Shen, H., Gong, J. & Xiao, Z. A comprehensive review on non-pneumatic tyre research. *Mater. Des.* **227**, 111742 (2023).
16. Sardinha, M., Fátima Vaz, M., Ramos, T. R. P. & Reis, L. Design, properties, and applications of non-pneumatic tires: A review. *Proc. Inst. Mech. Eng. Part L J. Mater. Des. Appl.* **237**, 2677–2697 (2023).
17. Dudziak, M., Lewandowski, A. & Waluś, K. J. Static tests the stiffness of car tires. *IOP Conf. Ser. Mater. Sci. Eng.* **776**, 012071 (2020).
18. Sonenblum, S. E., Sprigle, S. H. & Martin, J. S. Everyday sitting behaviour of full-time wheelchair users. *J. Rehabil. Res. Dev.* **53**, 585–598 (2016).
19. Koontz, A. M. et al. A kinetic analysis of manual wheelchair propulsion during start-up on select indoor and outdoor surfaces. *J. Rehabil. Res. Dev.* **42**, 447–458 (2005).
20. Wyatt, O., Chatzistergos, P., Pasiou, E. D., Chockalingam, N. & Ganniari-Papageorgiou, E. Exploration of the optimum finite element modelling techniques for honeycomb structures for non-pneumatic tyre applications. *Mater. Today Proc.* **93**, 743–747 (2023).
21. Ultimaker TPU 95A Technical data sheet, Ultimaker, https://um-support-files.ultimaker.com/materials/2.85mm/tds/TPU-95A/Ultimaker-TPU95A-TDS-v5.00.pdf (2022)
22. Aldhufairi, H. S. & Olatunbosun, O. A. Developments in tyre design for lower rolling resistance: A state of the art review. *Proc. Inst. Mech. Eng. Part D J. Automob. Eng.* **232**, 1865–1882 (2018).
23. Lin, C.-L., Chang, W.-J., Lin, Y.-S., Chang, Y.-H. & Lin, Y.-F. Evaluation of the relative contributions of multi-factors in an adhesive MOD restoration using FEA and the Taguchi method. Dent. Mater. 25, 1073–1081 (2009).
24. Chatzistergos, P. E., Naemi, R., Healy, A., Gerth, P. & Chockalingam, N. Subject specific optimisation of the stiffness of footwear material for maximum plantar pressure reduction. *Ann. Biomed. Eng.* **45**, 1929–1940 (2017).
25. Chatzistergos, P. E., Gatt, A., Formosa, C., Sinclair, J. K. & Chockalingam, N. Effective and clinically relevant optimisation of cushioning stiffness to maximise the offloading capacity of diabetic footwear. *Diabetes Res. Clin. Pract.* **204**, 110914 (2023).
26. Chatzistergos, P. E. & Chockalingam, N. A novel concept for low-cost non-electronic detection of overloading in the foot during activities of daily living. *R. Soc. Open Sci.* **8**, 202035 (2021).
27. Williams, E. et al. Perspectives of basic wheelchair users on improving their access to wheelchair services in Kenya and Philippines: A qualitative study. *BMC Int. Health Hum. Rights* **17**, 1–12 (2017).
28. Marchiori, C., Bensmail, D., Gagnon, D. & Pradon, D. Manual wheelchair satisfaction among long-term users and caregivers: A French study. *J. Rehabil. Res. Dev.* **52**, 181–192 (2015).
29. Veeramurthy, M., Ju, J., Thompson, L. L. & Summers, J. D. Optimisation of geometry and material properties of a non-pneumatic tyre for reducing rolling resistance. *Int. J. Veh. Des.* **66**, 193–216 (2014).
30. Ansys Help. Ansys Help. In Mechanical APDL User Guide. (2021).
31. Kim, K., Kim, D. M. & Ju, J. Static contact behaviors of a non-pneumatic tire with hexagonal lattice spokes. *SAE Int. J. Passeng. Cars Mech. Syst.* **6**, 1518–1527 (2013).
32. Aboul-Yazid, A. M., Emam, M. A. A., Shaaban, S. & El-Nashar, M. A. Effect of spokes structures on characteristics performance of non-pneumatic tires. *Int. J. Automot. Mech. Eng.* **11**, 2212–2223 (2015).
33. Kacker, R. N., Lagergren, E. S. & Filliben, J. J. Taguchi's Orthogonal Arrays Are Classical Designs of Experiments. J. Res. Natl. Inst. Stand. Technol. 96, 577–591 (1991).

34. Wyatt O, Chatzistergos P, Ganniari-Papageorgiou E, Chockalingam N. A Finite Element Investigation into the Tunability of Non-Pneumatic Tyres for Wheelchair Use. ISb2021 PC021, 784 (2021).
35. Mason, B. S., Van Der Woude, L. H. V. & Goosey-Tolfrey, V. L. The ergonomics of wheelchair configuration for optimal performance in the wheelchair court sports. *Sports Med.* **43**, 23–38 (2013).

Acknowledgements

This project was partially funded by the Engineering and Physical Sciences Research Council [grant number: EP/W00717/1] through TIDAL Network Plus—Transformative Innovation in the Delivery of Assisted Living Products and Services. Support from the Staffordshire Advanced Manufacturing Prototyping and Innovation Demonstrator (SAMPID), (partially funded by the European Regional Development Fund) is also acknowledged.

Author contributions

Panagiotis Chatzistergos (PC), Otis Wyatt (OW) and E. Ganniari-Papageorgiou (EGP) conceptualised the testing method. OW led the data collection and analysis with the support of PC and EGP. Nachiappan Chockalingam made a substantial contribution to the design of the testing methodology as well as to the interpretation of results. All authors were equally involved in writing this manuscript and approved the submitted version.

Declarations

Competing interests

The authors declare no competing interests.

Additional information

Supplementary Information The online version contains supplementary material available at https://doi.org/10.1038/s41598-024-79689-1.

Correspondence and requests for materials should be addressed to P.C.

Reprints and permissions information is available at www.nature.com/reprints.

Publisher's note Springer Nature remains neutral with regard to jurisdictional claims in published maps and institutional affiliations.